Trace metal cycling in the deep water of the South China Sea: The composition, sources, and fluxes of sinking particles

Tung-Yuan Ho,[a,b,*] Wen-Chen Chou,[c] Hui-Ling Lin,[d] and David D. Sheu[d]

[a] Research Center for Environmental Changes, Academia Sinica, Taipei, Taiwan
[b] Institute of Hydrological and Oceanic Sciences, National Central University, Jhongli, Taiwan
[c] Institute of Marine Environmental Chemistry and Ecology, National Taiwan Ocean University, Keelung, Taiwan
[d] Institute of Marine Geology and Chemistry, National Sun Yat-Sen University, Kaohsiung, Taiwan

Abstract

Moored sediment traps were deployed for 1 yr at depths of 120, 600, and 3500 m in the water column to investigate the trace metal (M) (Al, Ti, V, Cr, Mn, Fe, Co, Ni, Cu, and Zn) composition, sources, and fluxes of deep-water sinking particles. Vertical transport for most of the metals at 120 m was strongly associated with organic matter production, and the major part of many of the metals in the sinking particles was of anthropogenic origin. Although the lithogenic fraction in deeper waters greatly increased with depth, significant proportions of the nonlithogenic and nonintracellular fractions were still observed when using M : Al or M : P ratios as indicators, particularly for Zn, Cu, Ni, Co, and Mn. Because particles from horizontal transport and sediment resuspension are known to be lithogenic in the deep basin, the trace metals in sinking particles in the twilight zone and deep water, which feature significantly elevated M : Al ratios, originate from the downward transport of anthropogenic or authigenic origins. With increasing inputs from anthropogenic aerosols over large oceanic regions globally, the coupling and transport of some trace metals originating from anthropogenic aerosols, such as Zn, Cu, Co, and Ni, with sinking organic particles has become an important pathway for trace metal cycling not only in the euphotic zone, but also in the twilight zone and deeper waters.

Trace metals (M) play important roles as regulators and recorders of ocean processes (Bruland and Lohan 2003; Anderson and Henderson 2005). For example, Fe may become an important limiting factor for phytoplankton growth and influence ocean productivity and global climate (Martin 1990). Identifying processes that regulate the internal cycling of trace metals and quantifying their fluxes in the marine water column is vital to establishing these roles (Anderson and Henderson 2005). Particle transport in the marine water column is one of the most important forcings regulating the internal cycling of trace metals in the ocean (Turekian 1977; Whitfield and Turner 1987), which in turn controls the concentrations and availability of trace metals. In particular, sinking particles are dominant vehicles for transporting major and trace elements from oceanic surface waters to the twilight zone and deep waters (Pace et al. 1987; Pohl et al. 2004; Lamborg et al. 2008). Thus, the elemental composition, sources, and fluxes of sinking particles are essential pieces of information for understanding how major and trace elements are internally cycled in oceanic water columns (Bishop et al. 1977; Martin et al. 1987; Buesseler et al. 2007). In oceanic surface waters, biogenic particles serve as the predominant components of sinking particles in transporting materials from oceanic surface waters to deep waters. Previous field and culture studies have confirmed that intracellular trace metal quotas are relatively constant in phytoplankton assemblages (Bruland et al. 1991; Ho et al. 2003). Intracellular trace metal quotas in plankton assemblages are constrained to a range within

a factor of 2 to 3 for most bioactive trace metals (Ho 2006), which may be sufficiently constrained to compare these intracellular quotas to the composition of suspended and sinking particles in the marine water column to differentiate trace metal sources in the particles (Ho et al. 2007, 2010b).

Indeed, our recent study in the northern South China Sea observed that major amounts of trace metals in phytoplankton were adsorbed onto biogenic particles and phytoplankton (Ho et al. 2007). Thus, biogenic particles originating in surface waters serve as adsorbent agents that transport the metals to deep waters. We hypothesized that the enriched metals originate from anthropogenic aerosols that contain markedly soluble trace metals (Ho et al. 2007). To evaluate this hypothesis, we compared trace metal fluxes in the euphotic zone obtained from floating traps with aeolian-transported trace metal deposition fluxes estimated by aerosol deposition near the water sampling site in the South China Sea (Ho et al. 2010b). The study observed comparable composition and fluxes for 11 metals, Al, Ti, Mn, V, Co, Ni, Cu, Zn, Cd, Pb, and Ba, between the deposited aerosols and the sinking particles, demonstrating that aeolian-transported anthropogenic aerosols are the major source of many trace metals in surface waters (Ho et al. 2010b). Intracellular M : P quotas in marine phytoplankton become a useful indicator to evaluate trace metal sources in biogenic particles and sinking particles.

Aeolian input is an important trace metal source in the ocean, particularly in offshore oceanic regions. For example, the major source of iron in oceanic surface waters has been considered to be atmospheric transport (Jickells et al. 2005). Recent studies have suggested that anthropogenic aerosols (atmospherically suspended particles originating
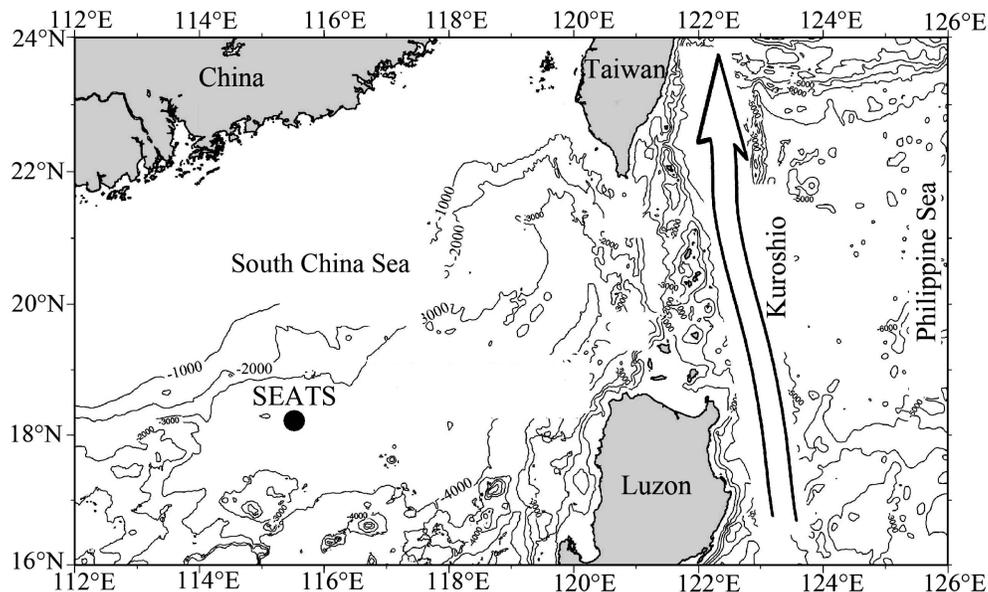
* Corresponding author: tyho@gate.sinica.edu.tw

Fig. 1. Location of the sampling site (115°34′E, 18°15′N) in the northern South China Sea.

from activities of humans, e.g., fossil fuel burning) may be the dominant source of soluble Fe in the ocean (Sedwick et al. 2007; Sholkovitz et al. 2009). Many other trace metals in aerosols are known to be of anthropogenic origin, such as Co, Cd, Cu, and Zn (Nriagu and Pacyna 1988). How anthropogenic aerosols quantitatively influence trace metal cycling in the marine water column still largely remains to be explored (Anderson and Henderson 2005). The South China Sea is adjacent to populous southern China, one of the most rapidly industrializing regions globally. Coal burning occupies a dominant role in Chinese fossil fuel consumption, accounting for one-third of global coal consumption. Satellite imaging shows that anthropogenic aerosols from fossil fuel and biomass burning originating in China and Southeast Asia are carried to this region throughout the year (Lin et al. 2007), suggesting a significant and steady input of aeolian-transported trace metals of anthropogenic origin in the region.

Following up on our previous findings about the importance of aeolian-transported anthropogenic aerosols as the major source of many trace metals in surface waters, we would like to answer the subsequent questions in this study. Have the trace metals of anthropogenic origin in the surface water reached the twilight zone and the deep water? How does trace metal composition in sinking particles vary with the input of the trace metals of anthropogenic origin? To further understand the internal cycling and transport of trace metals in sinking particles through the twilight zone and deep waters of the South China Sea, we have determined and evaluated the trace metal composition, sources, and vertical fluxes of sinking particles collected by moored sediment traps at depths of 120, 600, and 3500 m in the water column at the SouthEast Asian Time-Series station (SEATS), from August 2004 to October 2005. The major objective is to elucidate the mechanisms for trace metal cycling and transport in the water column.

Methods

Sampling site—The SEATS sampling site is located in the northern South China Sea basin and has a bottom depth of 3783 m (Fig. 1; Wong et al. 2007). The northern South China Sea experiences northeastern monsoons in winter and southwestern monsoons in summer. The seasonal primary production pattern has its highest production in winter and its lowest production in summer. Occasionally, strong winter monsoons may also induce dust storms that originate in the deserts of central China and carry lithogenic particles to surface waters (Lin et al. 2007). This semiclosed, deep-water basin also lies in a region surrounded by high fluvial inputs from land, mainly from the Pearl River next to the northern South China Sea and the Mekong River next to the southern South China Sea. Lateral transport of lithogenic particles from the continental margin may be significant.

Deployment of sediment traps—Time-series moored sediment traps were deployed at the station at depths of 120, 600, and 3500 m on two occasions. The first deployment lasted from 08 August 2004 to 16 February 2005; the second lasted from 01 April 2005 to 10 October 2005. Two types of French time-series sediment traps (Technicap Pièges à Particules Séquentiels, models 5/2 and 3/3) were used in the deployment, with 1.00- and 0.125-m² cone areas and 8- and 16-d collection intervals for each cup, respectively. The trap body and baffle material were made of reinforced polyester and phenolic composite, respectively. The trapping bottles were made of polypropylene and were acid washed before use. The trap solutions in the trap cups were prepared in an acid-washed polypropylene bottle by adding 800 g of Merck guarantee reagent grade NaCl to 20 liters of subsurface seawater taken near the trap deployment location in which trace metal concentrations

were known to be depleted (Wen et al. 2006; Norisuye et al. 2007). The total amounts of trace metals in the sinking particles collected in the traps were at least two orders of magnitude higher than those originating from the NaCl salts. Thus, contamination from the brine is negligible. After retrieving the traps, the sample bottles were detached, sealed, and stored in a cold room at 4°C on board the ship until further processing onshore.

Trace metal dissolution and desorption—An important analytical issue concerns particle dissolution and elemental desorption during the long-term storage of sinking particles collected in sediment traps. Significant amounts of trace metals and organic matter in sinking particles may become soluble through desorption and particle dissolution, even with Hg added in the trapping solution (Antia 2005; Liu et al. 2006). Hg is a commonly used poison to control microbial activity in trap studies, although it also causes the overestimation of particulate organic carbon (POC) due to the accumulation of zooplankton material in trap cups. Hg was not used in this trap study. It is thus essential to determine and include the soluble portion of trace metals in the supernatant collected in the trap cups to obtain accurate total fluxes (Knauer and Martin 1981). The salinity of the supernatants in the trap cups after collection was close to their original value, indicating that the exchange of the supernatant with ambient seawater was limited. We determined the amount of soluble trace metals in the supernatants. Supernatant samples were first diluted 100- or 1000-fold with element-grade Milli-Q water in acid-washed quartz tubes and then treated with 1200 W ultraviolet (UV) radiation for 12 h to decompose soluble organic matter. The diluted and UV-treated solution was ready for trace metal analysis after being filtered through 0.2-μm acid-washed polycarbonate filters. Significant amounts of some elements were present in the supernatant solution at 120 m, where adsorption activity and organic matter dissolution are supposed to be high. The portion in the supernatant relative to the total amount in the sample can occasionally be over 50% for some elements, including P, V, Cr, Mn, Co, Ni, Cu, and Zn. A significant fraction of some metals was also present in the supernatant for some samples at 600 m. To further validate the accuracy of our trace metal measurements, we compared the trace metal fluxes and composition of the sinking particles collected in this study with the data for suspended and sinking particles obtained from the two previous studies in surface waters (Ho et al. 2007, 2010*b*). Again, we obtained comparable and consistent values, validating the accuracy of our measurements. It is thus essential to measure the soluble trace metals in the supernatant of long-term trap samples to obtain accurate trace metal fluxes, particularly when working in the euphotic and twilight zones (Pohl et al. 2004; Antia 2005).

Pretreatment and analysis—In the onshore laboratory, the supernatant from each collection cup of the sediment traps was first transferred using a plastic syringe to acid-washed polypropylene bottles and stored in a refrigerator (2°C) until further processing. Particle samples were divided into six portions using a Perimatic peristaltic pump dispenser (Jencons). These subsamples were then passed through a 1-mm nylon mesh to remove swimmers and large zooplankton. Other swimmers that passed through the sieve were picked out manually using plastic tweezers. A small portion of well-mixed particles was sampled and filtered through a 0.2-μm acid-washed polycarbonate filter under low vacuum. After being freeze-dried, the filters were soaked in a mixture of 0.9 mL of ultra-pure nitric acid and 0.1 mL of ultra-pure hydrofluoric acid (Seastar) in 10-mL microwavable Teflon vials. The filters containing the sinking particles, along with blank filters, were digested in a MARS microwave oven (CEM) at 180°C for 15 min with a 10-min ramp from room temperature to 180°C. After complete digestion, the samples were evaporated to near dryness on hot plates at 80°C in a trace-metal–clean hood. The dried samples were combined with super-pure nitric acid and diluted sequentially with element grade Milli-Q water to obtain samples in a 3% nitric acid solution that were ready for inductively coupled plasma mass spectrometer (ICP-MS) analysis. The concentrations of all elements analyzed were determined with a sector field double-focusing high-resolution ICP-MS (Element XR, Thermo Scientific) equipped with a desolvation system (Elemental Scientific). The sensitivity and stability of the instrument were adjusted to optimal conditions before analysis. The detection limits of our high resolution ICP-MS for trace metals are generally at the low ng L^{-1} level. The concentrations in the digested samples and supernatant solution were generally too high, and thus the samples were diluted to decrease the concentrations to the low μg L^{-1} level before analysis. The trace metal concentrations in the diluted samples were almost all two orders of magnitude above the filter blank concentrations, which were below the μg L^{-1} level for all measured trace metals. The analysis was conducted with a sensitivity of approximately 10^6 counts s^{-1} for 1 μg L^{-1} indium, and analytical precision was generally between 1% and 2%. Twelve external and three internal standards (Sc, Y, and In) were used for accurate quantification. The plankton and seawater reference materials we have used are plankton certified reference material (CRM) 414 (Community Bureau of Reference, Commission of the European Communities) and reference seawater NASS-5 (National Research Council, Canada). The details of the analytical precision, accuracy, and detection limits of the methods for particle and seawater analysis are described in Ho et al. (2003, 2007, 2010*a*).

Results

Elemental fluxes: Temporal and vertical—The raw data and vertical and temporal variability of the elemental fluxes are presented in Tables 1, 2, and 3 and Fig. 2. The temporal variability of the elemental fluxes exhibits several different patterns at 120 m. P, Zn, Cu, and Mn show elevated fluxes in winter and spring from January to May and relatively low fluxes in summer from July to September, which is consistent with the temporal patterns of primary production (Chen 2005; Tseng et al. 2005). The temporal variability trends of V, Co, and Ni are similar to

Table 1. The raw data of the elemental fluxes (μmol m^{-2} d^{-1}) at 120 m.

Period	Al	P	Ti	V	Cr	Mn	Fe	Co	Ni	Cu	Zn
16 Aug 2004	12	89	0.62	0.014	0.038	0.11	2.9	0.002	0.067	0.12	0.52
01 Sep 2004	14	51	0.51	0.014	0.083	0.12	4.7	0.001	0.072	0.09	0.59
17 Sep 2004	44	122	1.75	0.050	0.054	0.13	5.1	0.005	0.154	0.11	1.52
03 Oct 2004	5	231	0.20	0.042	0.029	0.21	4.2	0.010	0.254	0.15	3.29
19 Oct 2004	25	280	0.76	0.060	0.077	0.24	8.1	0.015	0.299	0.29	4.29
04 Nov 2004	27	198	0.78	0.041	0.040	0.34	8.0	0.007	0.226	0.22	2.71
20 Nov 2004	4	82	0.14	0.019	0.005	0.19	1.7	0.003	0.103	0.13	0.87
06 Dec 2004	57	138	1.69	0.056	0.025	0.83	12.4	0.016	0.475	0.16	1.19
22 Dec 2004	34	161	0.86	0.053	0.052	0.36	8.7	0.009	0.206	0.29	1.93
07 Jan 2005	50	446	1.36	0.126	0.042	0.56	13.5	0.014	0.296	0.32	8.23
23 Jan 2005	24	516	1.05	1.062	0.084	0.95	7.6	0.024	0.665	0.88	21.35
08 Feb 2005	12	710	0.36	0.673	0.034	0.91	6.0	0.024	0.724	0.75	26.96
09 Apr 2005	0.31	1187	0.418	0.573	0.083	0.717	12.5	0.093	0.663	1.628	42.07
25 Apr 2005	5.40	772	0.181	3.151	0.210	0.634	25.7	0.305	1.211	2.600	41.98
11 May 2005	78.14	197	1.890	3.481	0.280	0.195	33.7	0.423	2.857	1.022	19.18
27 May 2005	7.20	183	0.409	3.346	0.021	0.105	13.4	0.395	2.219	1.326	20.37
12 Jun 2005	92.91	403	3.167	1.323	0.187	0.403	51.4	0.236	2.418	1.143	37.13
28 Jun 2005	4.25	235	0.225	0.020	0.001	0.024	1.9	0.021	0.404	0.082	1.163
14 Jul 2005	0.12	33	0.009	0.006	0.006	0.008	0.2	0.006	0.083	0.010	0.105
30 Jul 2005	4.83	166	0.231	0.026	0.002	0.050	4.3	0.029	0.643	0.132	1.800
15 Aug 2005	0.06	56	0.008	0.012	0.007	0.010	0.6	0.007	0.258	0.011	0.061
31 Aug 2005	0.05	46	0.004	0.007	0.003	0.006	0.2	0.007	0.283	0.005	0.053
16 Sep 2005	0.10	80	0.010	0.010	0.005	0.009	0.8	0.010	0.461	0.011	0.082
02 Oct 2005	0.49	157	0.008	0.006	0.004	0.006	0.4	0.007	0.317	0.009	0.054

the temporal variability of organic matter to some extent, but their fluxes were one order of magnitude higher from April to June than the fluxes in other seasons and did not match the season, with highest organic matter fluxes lasting from January to April. Vertically, the fluxes of the elements P, Zn, Cu, Ni, Co, and V generally decreased from 120 to 600 m (Fig. 2), indicating that these metals are remineralized during the decomposition of organic matter as the particles sink through the top 600 m of the water column. However, the fluxes of the typical, lithogenic-type trace metals, such as Al, Fe, Ti, Mn, and Cr, increased with depth from surface waters to the bottom traps (Fig. 2). Overall, averaged fluxes of Al were 21, 66, and 132 μmol m^{-2} d^{-1} from the 120, 600, and 3500 m traps, respectively. The other major lithogenic-type metals (i.e., Fe, Ti, and Cr) also exhibited similar temporal patterns with depth. The fluxes of these trace metals at 3500 m were approximately 2- to 4-fold greater than the middle traps. These lithogenic-type metals also exhibited similar temporal patterns at the deeper depths when compared to each other, with gradually increasing fluxes from December 2004 to February 2005 but gradually decreasing from April 2005 to October 2005. At 600 m, an abnormally elevated signal for almost all elements was recorded at the end of December, coinciding with the South Asia tsunami in 2004.

Discussion

Evaluation of POC fluxes—POC fluxes are vital information for material cycling in marine water columns. Although the accuracy of the estimated POC fluxes of the surface trap in this study is evaluated here, the major focus of this study lies in the twilight zone and the deep water,

and the central arguments presented are primarily based on elemental ratios instead of absolute fluxes. POC fluxes obtained from moored sediment traps can be significantly biased due to the interference of strong physical forcings with particle collection in oceanic surface waters (Buesseler 1991; Buesseler et al. 2007). Freely floating traps are generally considered to provide more accurate POC flux data than moored traps (Baker et al. 1988; Buesseler et al. 2007). At the SEATS site, we have obtained POC fluxes by using floating traps in the surface water on four occasions (Ho et al. 2010b). Nitrate-based new production information was also available at the same study site (Chen 2005). In brief, the POC fluxes estimated from sinking organic P obtained from the moored traps in this study were comparable to nitrate-based new production and the POC fluxes obtained by floating traps at SEATS (Chen 2005; Ho et al. 2010b).

The current velocities in the surface water at SEATS are generally low. The average zonal velocities (u and v) at 120 m in August (-4 and 4 cm s^{-1}) and December (-25 and -2 cm s^{-1}) were obtained from field current data averaged over the period from 1999 to 2003 (Wu et al. 2005). The pressure data from the current meters installed with the traps showed that the variability of the trap depth was limited. The averaged corresponding depths of the three traps with one standard deviation were 123 $\pm$ 17, 625 $\pm$ 6, and 3454 $\pm$ 2 m for the first deployment and 84 $\pm$ 31, 529 $\pm$ 6, and 3487 $\pm$ 0.8 m for the second deployment, respectively. The trap strings of this study were stretchable in seawater, so the effective depths may vary to some extent. The major cause of the depth variability is the effect of tidal currents, observed by the diurnal oscillation of the trap depths. Internal waves, which are substantial in the

Table 2. The raw data of the elemental fluxes (μmol m^{-2} d^{-1}) at 600 m.

Period	Al	P	Ti	V	Cr	Mn	Fe	Co	Ni	Cu	Zn
12 Aug 2004	15	4	0.42	0.018	0.015	0.34	3.9	0.002	0.061	0.03	0.12
20 Aug 2004	18	9	0.56	0.018	0.018	0.28	4.7	0.003	0.064	0.03	0.18
28 Aug 2004	20	14	0.57	0.019	0.025	0.19	4.4	0.002	0.053	0.04	0.19
05 Sep 2004	23	4	0.69	0.024	0.022	0.23	5.5	0.003	0.066	0.10	0.18
13 Sep 2004	28	9	0.78	0.031	0.021	0.54	7.5	0.004	0.108	0.05	0.16
21 Sep 2004	28	8	0.85	0.028	0.015	0.57	7.5	0.005	0.101	0.05	0.16
29 Sep 2004	30	5	0.87	0.035	0.020	0.65	7.7	0.005	0.098	0.04	0.14
07 Oct 2004	31	6	0.90	0.033	0.020	0.58	8.2	0.005	0.099	0.04	0.14
15 Oct 2004	46	16	1.25	0.043	0.034	0.71	12.1	0.007	0.161	0.07	0.23
23 Oct 2004	30	12	0.93	0.035	0.023	0.46	8.4	0.006	0.131	0.08	0.32
31 Oct 2004	124	12	3.71	0.116	0.086	1.13	31.1	0.014	0.312	0.38	0.51
08 Nov 2004	57	9	1.70	0.052	0.033	0.60	14.1	0.007	0.145	0.05	0.20
16 Nov 2004	31	5	0.91	0.034	0.019	0.45	8.4	0.004	0.093	0.05	0.12
24 Nov 2004	26	12	0.76	0.024	0.014	0.38	7.0	0.003	0.074	0.03	0.10
02 Dec 2004	55	18	1.53	0.056	0.027	1.07	14.3	0.008	0.189	0.08	0.34
10 Dec 2004	68	9	2.07	0.067	0.045	0.70	17.4	0.008	0.171	0.07	0.18
18 Dec 2004	215	18	6.49	0.192	0.133	1.95	52.8	0.023	0.449	0.23	0.42
26 Dec 2004	332	43	9.11	0.258	0.170	2.50	79.3	0.030	0.582	0.08	0.38
03 Jan 2005	115	34	3.47	0.101	0.075	1.13	28.3	0.013	0.251	0.09	0.73
11 Jan 2005	119	40	4.22	0.133	0.085	1.50	28.7	0.016	0.477	0.19	1.03
19 Jan 2005	169	11	4.96	0.166	0.094	1.50	43.8	0.018	0.368	0.07	0.26
27 Jan 2005	148	11	4.29	0.140	0.089	1.76	37.1	0.016	0.317	0.10	0.23
04 Feb 2005	103	8	2.89	0.096	0.062	0.99	25.3	0.012	0.219	0.05	0.18
12 Feb 2005	101	8	2.94	0.097	0.060	1.10	25.1	0.012	0.228	0.06	0.18
09 Apr 2005	52	26	1.339	0.059	0.029	0.345	14.8	0.024	0.166	0.089	0.222
25 Apr 2005	46	24	1.163	0.049	0.024	0.314	12.7	0.019	0.264	0.051	0.148
11 May 2005	46	23	1.162	0.049	0.025	0.313	13.1	0.023	0.186	0.058	0.187
27 May 2005	32	27	0.754	0.034	0.017	0.188	8.5	0.019	0.159	0.035	0.154
12 Jun 2005	24	12	0.618	0.028	0.019	0.139	6.7	0.022	0.107	0.036	0.143
28 Jun 2005	33	24	0.906	0.034	0.023	0.152	9.1	0.018	0.141	0.072	0.172
14 Jul 2005	18	42	0.470	0.021	0.014	0.126	4.8	0.015	0.085	0.029	0.161
30 Jul 2005	22	26	0.589	0.023	0.021	0.145	5.7	0.014	0.090	0.029	0.150
15 Aug 2005	9	11	0.245	0.012	0.013	0.070	2.8	0.017	0.067	0.027	0.090
31 Aug 2005	27	12	0.745	0.029	0.024	0.151	7.6	0.017	0.113	0.034	0.160
16 Sep 2005	25	38	0.701	0.032	0.027	0.109	6.7	0.028	0.094	0.088	0.960
02 Oct 2005	103	14	3.000	0.096	0.075	0.646	25.9	0.029	0.236	0.069	5.251

northern South China Sea, may be other physical forces that influence the variability of the trap depths and tilt.

Although POC in the sinking particle samples was also measured by the other research group, the POC data were likely to be significantly underestimated due to the dissolution problem. Based on the study of Antia (2005) and on what we found for excess P in the supernatant in the surface water (Table 4), a significant amount of sinking POC collected in oceanic surface water dissolved in the supernatant, particularly in the shallow depth. It is thus essential to determine the soluble component in supernatant to obtain representative total fluxes in the surface trap (Antia 2005). In this study, we used two distinct methods, spectrophotometer and ICP-MS, to determine the soluble P in the supernatant and obtained comparable data (Ho et al. 2009). Since P was measured both in the supernatant and in sinking particles, the organic particulate P data are relatively representative and reliable. However, the soluble carbon portion from sinking particles in the supernatant was not determined. Significant unknown amounts of POC were likely decomposed to dissolved organic carbon and dissolved inorganic carbon and then were respired to carbon dioxide after long-term storage because we did not

add Hg in the trap cups. The averaged C:P molar ratios, using particulate POC only and our total organic P data, are 16 ± 7, 37 ± 16, and 66 ± 26, respectively, for all samples in the three traps from top to bottom in the first deployment. Particulate inorganic P concentrations were subtracted in the calculation by using 0.1% of inorganic P to lithogenic Al ratio in lithogenic particles. Similarly, by using the particulate POC data without supernatant portion, we found that the particulate-only POC data in the surface trap were also much lower than previous available POC data at SEATS. The fluxes in October were around 2 mmol m^{-2} d^{-1}, only about one-fifth of the fluxes obtained by floating trap (Ho et al. 2010b). Thus, POC fluxes that do not include a correction for degradation and dissolution, as indicated by analysis of the supernatant (Table 4), are underestimates, with shallower traps more prone than deeper ones.

Although particulate organic P is preferentially regenerated from sinking particulate organic matter in the oceanic water column, C:P ratios in sinking organic particles are still close to the Redfield ratio in the upper ocean if total particulate materials are measured (Antia 2005). The total particulate materials include both the particulate material

Table 3. The raw data of the elemental fluxes (μmol m^{-2} d^{-1}) at 3500 m.

Period	Al	P	Ti	V	Cr	Mn	Fe	Co	Ni	Cu	Zn
12 Aug 2004	177	6.3	4.50	0.154	0.087	2.18	43.2	0.022	0.304	0.19	0.14
20 Aug 2004	119	5.1	3.24	0.110	0.063	1.70	29.5	0.017	0.224	0.09	0.14
28 Aug 2004	111	4.9	2.87	0.102	0.054	1.63	27.2	0.017	0.203	0.09	0.15
05 Sep 2004	77	3.8	2.11	0.077	0.042	1.22	19.0	0.013	0.152	0.07	0.11
13 Sep 2004	77	5.2	1.97	0.073	0.042	1.20	18.6	0.012	0.126	0.09	0.19
21 Sep 2004	68	3.3	1.84	0.068	0.036	1.19	16.9	0.012	0.136	0.12	0.16
29 Sep 2004	85	4.0	2.24	0.083	0.045	1.35	20.8	0.017	0.162	0.08	0.18
07 Oct 2004	126	5.4	3.18	0.114	0.060	2.11	31.0	0.023	0.229	0.10	0.20
15 Oct 2004	115	5.6	3.14	0.111	0.059	2.03	28.4	0.022	0.225	0.14	0.18
23 Oct 2004	153	6.9	4.05	0.144	0.079	2.80	37.9	0.030	0.293	0.15	0.19
31 Oct 2004	114	6.0	3.20	0.116	0.061	2.27	28.3	0.023	0.240	0.12	0.16
08 Nov 2004	86	4.5	2.49	0.088	0.063	1.67	21.1	0.017	0.184	0.09	0.16
16 Nov 2004	92	4.4	2.41	0.091	0.046	1.82	23.6	0.019	0.187	0.09	0.11
24 Nov 2004	90	4.2	2.47	0.095	0.043	1.89	23.9	0.018	0.193	0.09	0.11
02 Dec 2004	101	4.8	2.72	0.107	0.049	2.16	26.6	0.021	0.215	0.13	0.14
10 Dec 2004	183	11.4	4.86	0.187	0.091	3.90	48.0	0.044	0.398	0.20	0.35
18 Dec 2004	158	7.6	4.07	0.148	0.078	2.63	39.7	0.028	0.299	0.12	0.17
26 Dec 2004	201	9.1	5.30	0.188	0.097	3.01	50.1	0.033	0.381	0.14	0.20
03 Jan 2005	173	7.7	4.76	0.166	0.088	2.65	43.1	0.029	0.336	0.13	0.29
11 Jan 2005	222	8.8	5.68	0.199	0.106	2.97	55.0	0.032	0.395	0.13	0.19
19 Jan 2005	204	8.0	5.35	0.182	0.101	2.48	50.0	0.027	0.358	0.10	0.18
27 Jan 2005	300	11.5	7.84	0.261	0.145	3.52	74.8	0.040	0.518	0.17	0.25
04 Feb 2005	256	10.0	6.97	0.228	0.125	3.14	62.7	0.035	0.459	0.14	0.22
05 Apr 2005	144	6.3	3.54	0.12	0.069	1.9	36	0.020	0.249	0.09	0.136
13 Apr 2005	150	8.7	3.62	0.13	0.070	2.1	37	0.026	0.268	0.09	0.150
21 Apr 2005	128	7.2	3.10	0.12	0.061	2.0	32	0.022	0.241	0.09	0.143
29 Apr 2005	146	7.5	3.61	0.13	0.072	2.1	36	0.025	0.269	0.10	0.200
07 May 2005	223	10.0	5.49	0.20	0.104	3.2	55	0.031	0.390	0.13	0.287
15 May 2005	185	8.8	4.56	0.17	0.087	2.6	46	0.027	0.331	0.19	0.227
23 May 2005	135	7.6	3.41	0.12	0.070	2.1	34	0.023	0.256	0.10	0.282
31 May 2005	115	7.6	2.89	0.10	0.059	1.9	28	0.022	0.221	0.10	0.229
08 Jun 2005	119	6.3	3.00	0.11	0.060	2.1	29	0.021	0.224	0.11	0.261
16 Jun 2005	124	6.3	3.13	0.12	0.065	2.1	31	0.023	0.240	0.10	0.155
24 Jun 2005	143	7.8	3.53	0.13	0.073	2.4	35	0.024	0.271	0.11	0.287
02 Jul 2005	106	6.2	2.64	0.10	0.055	2.0	27	0.021	0.208	0.09	0.245
10 Jul 2005	126	7.1	3.16	0.12	0.064	2.3	31	0.023	0.241	0.11	0.191
18 Jul 2005	90	6.3	2.25	0.08	0.046	1.6	22	0.019	0.173	0.08	0.153
26 Jul 2005	95	9.0	2.34	0.09	0.049	1.8	23	0.020	0.185	0.09	0.128
03 Aug 2005	109	9.7	2.66	0.10	0.054	2.0	27	0.020	0.208	0.10	0.132
11 Aug 2005	111	6.2	2.67	0.10	0.057	1.8	26	0.021	0.203	0.10	0.149
19 Aug 2005	107	9.9	2.61	0.10	0.054	1.9	27	0.021	0.203	0.09	0.166
27 Aug 2005	90	10.1	2.70	0.10	0.055	2.0	22	0.023	0.210	0.10	0.164
04 Sep 2005	113	8.8	2.80	0.10	0.056	2.1	28	0.022	0.216	0.10	0.163
12 Sep 2005	86	4.9	2.09	0.08	0.044	1.7	21	0.017	0.172	0.09	0.158
20 Sep 2005	74	5.0	1.91	0.07	0.043	1.5	18	0.017	0.152	0.08	0.151
28 Sep 2005	111	6.6	2.74	0.11	0.055	2.1	28	0.023	0.219	0.11	0.143
06 Oct 2005	74	4.4	1.92	0.07	0.041	1.4	19	0.016	0.159	0.08	0.094

in traps cups and the dissolved portion in the supernatant that originates from particulate material. The study of Antia (2005) compiled the results of 13 studies measuring C, N, and P concentrations in sinking particulate material collected by sediment traps. Eight of the studies measured only particulate material in the trap cups, and four of the studies measured total material in the trap cups. Two-thirds of C:P ratios in the particulate-only samples in depths above 1000 m ranged from 300 to 900, most likely due to preferential P dissolution. In the other four studies measuring total material in the sinking particles in the upper ocean, the C:P ratios ranged from 88 to 131 in water depths shallower than 1000 m, and the ratios varied from 187 to 236 in depths between 1000 and 4000 m. This result indicates that C:P ratios in sinking organic particles are close to the Redfield ratio in the upper ocean if total particulate material is measured. Similarly, in the South China Sea, the C:P ratio in sinking particles collected by floating traps deployed for 1 to 2 d in the top 160 m was 109 (Ho et al. 2010b), also showing that the ratios are close to the Redfield ratio. Based on the study of Antia (2005) and our floating trap data in the surface water at SEATS, the estimated POC fluxes from the total P data of this study in the surface water are assumed to be within 30% of total
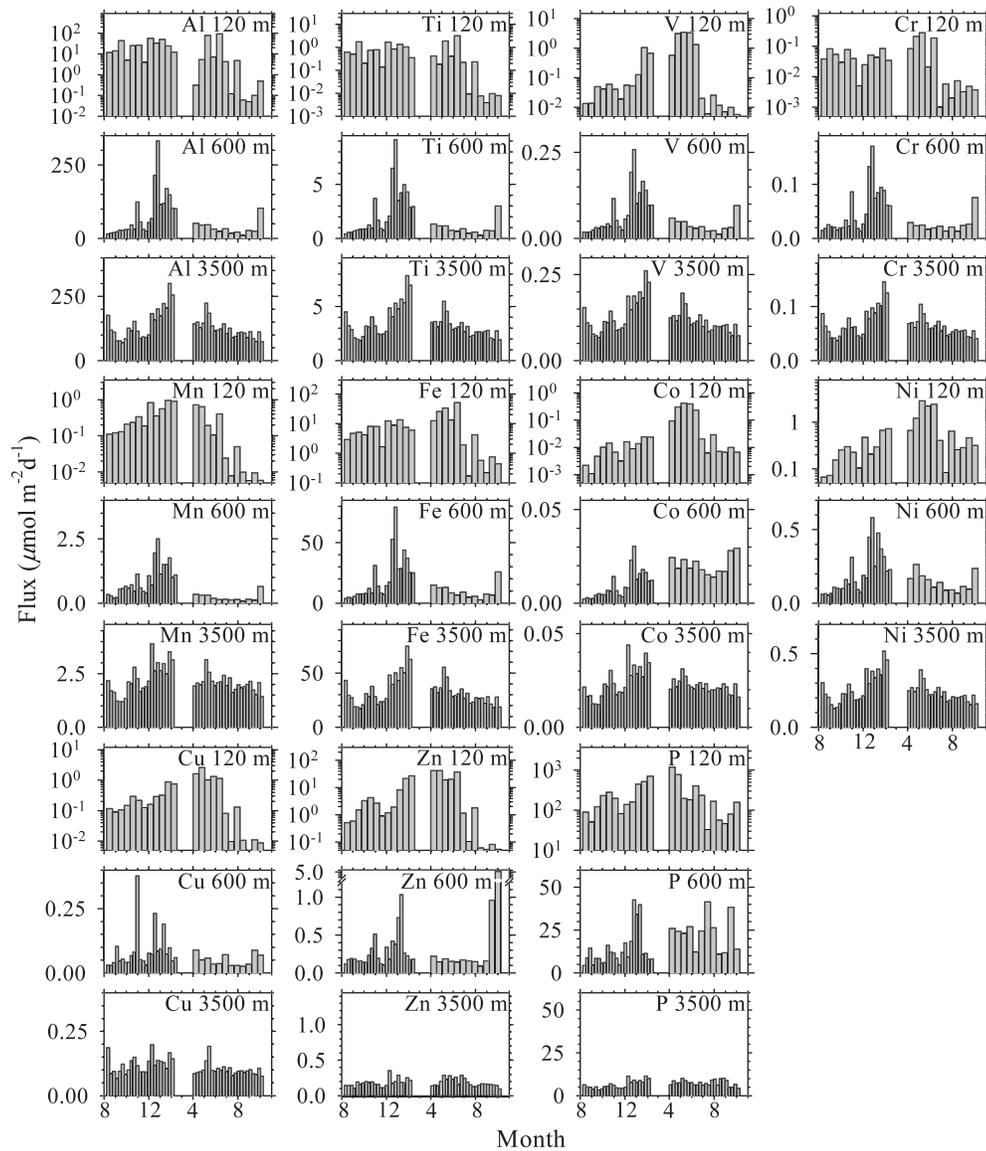
Fig. 2. The elemental fluxes at depths of 120, 600, and 3500 m at the SEATS site from August 2004 to October 2005. Each deployment lasted for 6 months. The fluxes at 120 m are shown with a log scale, and the scales of the two deeper depths are formatted to be the same for each element.

POC fluxes by using the Redfield conversion. This 30% variability is an insignificant portion compared to the possible variability for POC flux studies (Buesseler 1991; Buesseler et al. 2007). Thus, we take the POC fluxes estimated from total organic P in the surface water to be meaningful.

The reported nitrate-based new production in the top 100 m of the SEATS site ranged from 0.03 to 0.07 g C m^{-2} d^{-1} during the summer and fall seasons and was up to 0.26 g C m^{-2} d^{-1} during winter (Chen 2005). The new production values reported by Chen (2005) in March were low, ranging only from 0.06 to 0.07 g C m^{-2} d^{-1}. The vertical POC fluxes obtained by using floating traps at 100 m were 0.15, 0.16, and 0.21 g C m^{-2} d^{-1} for three sampling events in January 2007, October 2006, and

October 2007, respectively, and 0.12 g C m^{-2} d^{-1} for one event in July (Ho et al. 2010b). The estimated POC fluxes by using total organic phosphorus data in the 120-m sediment traps (Table 1) ranged from 0.04 to 1.5 g C m^{-2} d^{-1} throughout the year, as follows: an average of 0.10 ± 0.06 g C m^{-2} d^{-1} during the summer months of July to September, a range of 0.10 to 0.66 g C m^{-2} d^{-1} with an average of 0.33 ± 0.19 g C m^{-2} d^{-1} during the winter months of October to January, and a range of 0.10 to 1.5 g C m^{-2} d^{-1} with an average of 0.55 ± 0.45 g C m^{-2} d^{-1} from October to April. The averaged POC fluxes obtained by moored surface traps during summertime were comparable to the two previous studies, with variability within a factor of 2. The estimated averaged POC fluxes obtained by moored surface traps during winter season were about 2-

Table 4. The percentage and standard deviation of the soluble elements in the supernatant to the total fluxes (particulate plus supernatant) for the two deployments (KK3: August 2004 to February 2005; KK4: April 2005 to October 2005).

Deployment	Depth (m)	Al	P	Ti	V	Cr	Mn	Fe	Co	Ni	Cu	Zn	Cd	Ba
KK3	120	0±0	58±16	1±1	49±24	16±18	69±21	13±15	45±18	44±18	22±15	21±16	33±23	15±14
	600	0±0	32±17	0±0	7±7	1±1	59±12	1±1	10±9	4±5	6±6	10±7	48±23	9±4
	3500	0±0	8±2	0±0	5±2	1±0	0±0	0±0	0±0	1±0	5±9	9±4	59±13	5±1
KK4	120	13±17	53±32	7±9	50±45	46±38	26±25	1±2	83±18	70±33	2±2	6±8	60±38	13±19
	600	0±0	63±14	0±0	18±7	19±7	3±2	5±2	80±8	35±14	3±1	8±4	99±1	0±0
	3500	0±0	15±10	0±0	2±0	3±1	0±0	0±0	14±5	3±1	0±0	3±2	98±3	1±4

fold of floating trap data in January and about 8-fold of the new production data obtained in March. It should be noted that the nitrate-based and floating trap methods were both carried out by research vessels on a daily basis, weather permitting. Primary production is about 2-fold higher during winter and spring seasons than in the summer season (Tseng et al. 2005). During the winter and spring seasons, the two previous flux studies likely missed the periods with elevated POC fluxes when strong storms occur. Overall, considering the analytical and sampling uncertainties between these three independent flux studies, the estimated POC fluxes obtained by the moored shallow sediment traps are relatively reliable. Without additional constraining data, we must take the two deeper traps to be at least as accurate as the shallow one.

Elemental correlation—The elemental correlation was further evaluated by principal component analysis (PCA). PCA identifies the common major components potentially influencing the variability of the fluxes; it also exhibits the flux correlation among different elements. For the first deployment, the total variances explained by PC1 are 61% (120 m), 75% (600 m), and 80% (3500 m) and for PC2 are 23%, 16%, and 9% for the three depths, respectively; for the second deployment, the variances explained by PC1 are 67%, 73%, and 75% and for PC2 are 21%, 16%, and 10% for the three depths, respectively. When the locations of the elements are together in the PCA plot, it means that their correlations are strong. Figure 3 shows that the temporal patterns for most of the trace metals at 120 m exhibit consistent variability with organic P or POC flux. The flux correlation coefficients between the trace metals and P at 120 m for the first deployment were 0.95, 0.89, 0.88, 0.86, 0.79, and 0.76 for Zn, Cu, Co, Ni, V, and Mn, respectively, all with statistical *p*-values less than 0.01. The temporal variability of trace metal fluxes is consistent with our previous findings that trace metals in both phytoplankton and sinking particles in surface waters were mostly nonintracellular and adsorbed onto biogenic particles (Ho et al. 2007, 2010*b*). A similar result was observed that trace metal fluxes in the surface water of the Baltic Sea were associated with seasonal mass fluxes either for biogenic or lithogenic particles (Pohl et al. 2004). In the two deeper depths, the variability of the fluxes at 600 and 3500 m can mostly be explained by lithogenic particles, as indicated by the strong correlation between Al and other metals shown in the PCA (Fig. 3). The fraction of inorganic P in

lithogenic particles also significantly increased with depth. The variability of the fluxes was thus associated with organic matter fluxes in the surface water. In contrast, the variability of lithogenic particles was the strongest influence on the variability of trace metal fluxes in the two deeper depths.

Our previous studies also observed that Al concentrations in suspended and sinking particles in surface waters increased with depth at the SEATS site during other years (Ho et al. 2007, 2010*b*). Lithogenic particles in the sediments may be stirred up and resuspended to the water column due to the disturbance of deep-water currents or other physical forcings in the deeper water. In addition to the sediment resuspension of lithogenic particles and horizontal input from the continental shelf or break, lateral transport through deep-water circulation may be another possible source of lithogenic particles in the northern South China Sea. The deep-water flow in the South China Sea may be from the western Philippines Sea (Qu et al. 2006). Periodic internal waves in these waters might also be an important physical forcing that enhances the resuspension of fine lithogenic particles in the deep water. Overall, the influence of lithogenic particles on metal composition and fluxes increases with depth in the water column (Figs. 2, 3). The lithogenic particles are not prone to decomposition in the water column but may scavenge elements like P or particle-reactive trace metals (Ho et al. 2009).

Because V, Ni, and Co can be good indicators of anthropogenic aerosols derived from heavy oil burning or coal burning (Nriagu and Pacyna 1988; Sedwick et al. 2007; Sholkovitz et al. 2009), their elevated fluxes from April to June possibly originate from the similar regional source of fossil fuel burning (Fig. 3). Regional anthropogenic activities, such as fossil fuel burning by fishing vessels, cargo ships, and tankers, may be potentially important surface-water aerosol sources of V, Ni, and Co during the summer season. In addition, Fe and Cr both show slightly elevated fluxes at surface depth from April to June in 2005. With the exception of Al and Ti, almost all of the trace metal fluxes in the surface waters of the South China Sea are associated with organic matter fluxes to some extent, similar to observations in other oceanic regions (Deuser et al. 1983; Jickells et al. 1984).

Early open-ocean studies observed that biogenic and lithogenic particles were strongly associated with one another in sinking particles throughout the whole water column (Honjo 1982; Deuser et al. 1983). Our study shows
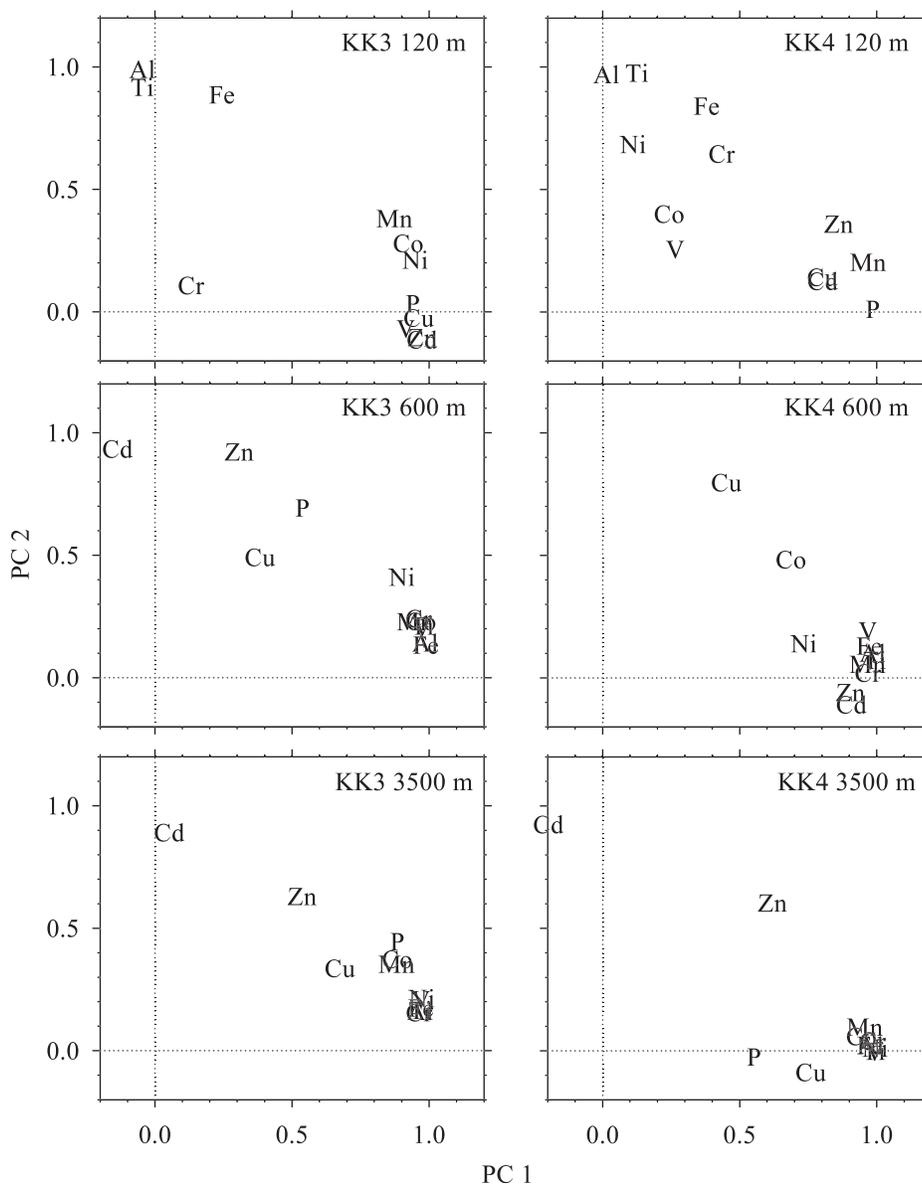
Fig. 3. Principal component analysis of the elemental fluxes of Al, P, Ti, V, Cr, Mn, Fe, Co, Ni, Cu, Zn, and Cd, at the three depths. KK3 and KK4 stand for the first and second deployment of the moored traps, respectively. PC1 stands for principal component 1, and PC2 stands for principal component 2. For the first deployment, the total variances explained by PC1 are 61% (120 m), 75% (600 m), and 80% (3500 m) and those explained by PC2 are 23%, 16%, and 9% for the three depths, respectively; for the second deployment, the variances explained by PC1 are 67%, 73%, and 75% and for PC2 are 21%, 16%, and 10% for the three depths, respectively.

that the fluxes of lithogenic-type metals are not associated with organic matter fluxes during the majority of the sampling time in deep waters (Fig. 3). The insignificant correlation between lithogenic-type metals, such as Al and Ti, and organic matter suggests that most lithogenic particles were not adsorbed onto biogenic particles but rather sank separately in deep waters. In contrast, trace metals of anthropogenic origin in surface waters, such as Zn and Cu, were mostly adsorbed onto organic matter and sank together. The input of trace metals of anthropogenic origin from atmospheric input and the lateral input of

sediment particles contribute to the individual metal content of the sinking particles; their relative contributions vary at different depths according to their relative proportions in the particles and the metal concentrations of the original source.

Trace metal composition and sources—Sources of trace metal in sinking particles can be divided into three basic categories: lithogenic, intracellular, and adsorbed. The intracellular component is defined as the trace metals that are incorporated into biota intracellularly. For assemblages

of phytoplankton in the euphotic zone of offshore oceanic regions, using intracellular M:P ratios to evaluate trace metal sources in biogenic suspended and sinking particles is valuable (Ho et al. 2007, 2010*b*). Early reliable field and culture studies have confirmed that trace metal quotas are relatively constant in phytoplankton assemblages. Intracellular trace metal quotas are within a factor of 2 or 3 among the field and laboratory studies (Ho 2006), which is sufficiently constrained to compare these quotas to the composition of biogenic particles in the field. The standard deviations of the intracellular quotas obtained from the field and laboratory studies (Ho 2006) are shown in the caption of Fig. 4 for reference. Because the Redfield ratio has historically been expressed as a normalized value of C and N to P, previous field and culture studies have generally expressed trace metal composition in marine plankton assemblages as a value normalized to P (Collier and Edmond 1984; Bruland et al. 1991; Ho et al. 2003). Therefore, the fluxes determined here were also presented as values normalized to phosphorus for comparison with previous intracellular metal quotas (Fig. 4). Because POC fluxes may be reasonably estimated by total P, assuming 30% variability in the surface water and a factor of 2 in the deep water, the M:P ratios obtained in the surface water and the deep water are useful indicators to evaluate the sources of trace metal in the sinking particles when the M:P ratios in the total sinking particulate material were generally 1–2 orders of magnitude higher than intracellular metal quotas in phytoplankton (Ho et al. 2007, 2010*b*). The M:P ratios obtained in the surface traps of this study are comparable to the previous studies, which include sinking particles collected by short-term floating traps (Ho et al. 2010), suspended particles collected by in situ pump filtration (Ho et al. 2007), and samples of live plankton collected by a novel plankton separation apparatus with gravity (Ho et al. 2007). All of the particles exhibited highly enriched metal quotas for most of the metals studied in the surface water, validating the M:P data obtained by moored traps in this study (Fig. 4). The approach of using M:P ratios to differentiate the sources of trace metals in sinking particles is useful.

Given the known intracellular trace metal composition in plankton and trace metal composition in lithogenic particles (Taylor 1964; Ho 2006), the relative contribution of the intracellular trace metals and trace metals in lithogenic particles to the sinking particles can be evaluated (Ho et al. 2007). We express their quantitative relationship by the following mass balance formula:

$$[M] = a[P] + b[Al]$$

where [M] (or M) is the total mass of a metal in particles; [P] (or P) is the intracellular phosphorus mass in biogenic organic particles; [Al] (or Al) is the aluminum mass in lithogenic particles; a is the P-normalized trace metal quota in plankton (Fig. 4); and b is the Al-normalized metal quota in lithogenic particles (Fig. 5).

The metal quotas of the samples are expressed by plotting the ratios of M:P or M:Al against the known stoichiometric constant a (Ho 2006) and constant b (Taylor

1964; Calvert et al. 1993), which are shown as the horizontal dashed lines for comparison in the plots of Figs. 4 and 5. P-normalized ratios for most of the metals at 120 m are significantly above the known intracellular metal quotas in plankton assemblages (Fig. 4). For example, Zn quotas ranged from 10 to 100 mmol mol^{-1} P, and Fe quotas ranged from 10 to 200 mmol mol^{-1} P. The ratios of both metals are much higher than their averaged intracellular quotas in marine plankton of 0.8 and 7.5 mmol mol^{-1} P, respectively (Ho et al. 2003; Ho 2006). In addition to Zn and Fe, all of the other trace metals also exhibited significantly elevated M:P ratios in comparison with their intracellular quotas in marine plankton. These significantly enriched metal quotas in the sinking particles indicate that most of the metals were nonintracellular and adsorbed onto the biogenic particle surfaces in surface waters (Fig. 3). This is consistent with our findings in the suspended marine phytoplankton assemblages and sinking particles of surface waters (Ho et al. 2007, 2010*b*). The only exception to this trend is the metal Cd, which was primarily integrated into biogenic organic matter (Ho et al. 2009). The P-normalized ratios for Zn, Cu, V, Ni, and Co varied significantly and exhibited elevated ratios in the surface traps from April to June 2005 (Fig. 4). The M:P ratios at the two deeper traps were still significantly higher than the known stoichiometric constant a, but the temporal variability of the ratios was relatively small mainly because of the increase of lithogenic particles in the deeper water.

The M:Al ratios are presented in Fig. 5. The dashed lines in the figure represent the element:Al ratios of the lithogenic particles obtained from the study of Calvert et al. (1993), which are shown in brackets for each element as follows: Ti (20), V (0.88), Cr (0.58), Mn (5.7), Fe (252), Co (0.18), Ni (0.32), Cu (0.49), Zn (0.54), and P (8.3) mmol mol^{-1} Al. The sediment sampling site, labeled as the station name (GGC) 1, was located at 117°50′E, 14°00′N, the site most adjacent to SEATS in the study (*see* table 1 in Calvert et al. 1993). We believe the M:Al ratios obtained in the sediment well represent the M:Al ratios of the suspended lithogenic particle around the northern South China Sea because almost all of the lowest M:Al ratios observed in our study are close to the M:Al ratios in the sediment, except Ni. The Ni:Al ratio of the lithogenic particles, shown as 0.32 mmol mol^{-1} Al in Figs. 5 and 6, might be underestimated, and, thus, the lithogenic fraction of Ni in deep water might be underestimated too.

At 120 m, the M:Al ratios of the sinking particles also varied significantly with time (Fig. 5). The ratios for many of the trace metals in surface waters were significantly higher than their crustal ratios during the majority of the sampling time (Fig. 5). In particular, the M:Al ratios of Zn and Cu at 120 m can be up to several orders of magnitude higher than their crustal ratios. Temporal variability at the two deeper traps was much less than at the surface trap, and their ratios were much closer to their crustal ratios, which is attributed to the increasing contribution of lithogenic particles with depth. The M:Al ratios of sinking particles were fairly constant for Fe and Ti at 600 m and for Fe, Ti, V, and Cr at 3300 m. Their ratios are almost the same as or very close to the M:Al ratio in lithogenic
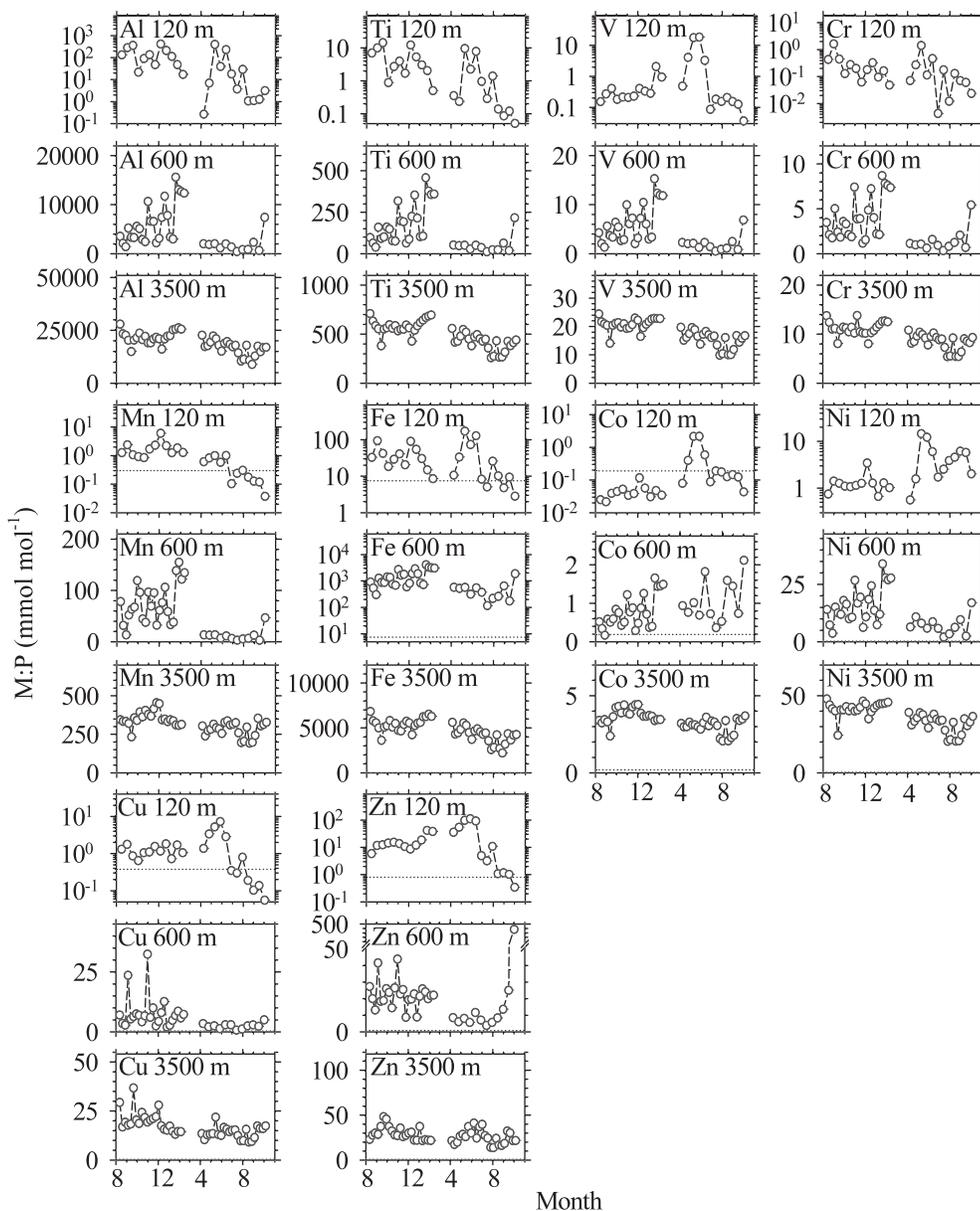
Fig. 4.   P-normalized elemental ratios of the sinking particles collected at depths of 120, 600, and 3500 m at the SEATS site from August 2004 to October 2005. The horizontal dashed lines represent the intracellular quota in marine plankton assemblages (Ho 2006), which are shown in brackets with one standard deviation for each element as follows: Mn (0.68 ± 0.54), Fe (5.1 ± 1.6), Co (0.15 ± 0.06), Ni (0.70 ± 0.54), Cu (0.41 ± 0.16), and Zn (2.1 ± 0.88) mmol mol^{-1} P. The standard deviations were estimated by using the field and culture studies (Collier and Edmond 1984; Bruland et al. 1991; Kuss and Kremling 1999; Ho et al. 2003).

particles, indicating that most of these elements in deep waters originated from lithogenic particles (Fig. 5). Fe exhibits a particularly strong linear correlation with Al at 3500 m with a slope of 0.253 mol mol^{-1} Al (Fig. 6), which is analytically the same as the Fe : Al ratio of 0.252 mol mol^{-1} Al observed in the sediment. In addition, the intercepts of the linear regression lines between Fe and Al fluxes at the two deeper depths pass through zero when the Al flux is extrapolated to zero, showing that almost all Fe in the sinking particles was from lithogenic particles. Similar results are observed for Ti, V, and Cr in the deep

water. Nevertheless, the temporal variability of the ratios for Mn, Co, Ni, Cu, and Zn were enormous at 600 m. Even though the M : Al ratios greatly decreased with depth due to an increasing contribution from lithogenic particles, the M : Al ratios at the two deeper traps for the metals Mn, Co, Ni, Cu, and Zn are still significantly higher than the M : Al ratios (Fig. 5). Especially, the Cu : Al and Zn : Al ratios were even still one order of magnitude higher than their composition in the lithogenic sediments. Although the ratios of Zn : Al in the sinking particles at times approached crustal values at 3500 m, they were up to 4-fold greater than
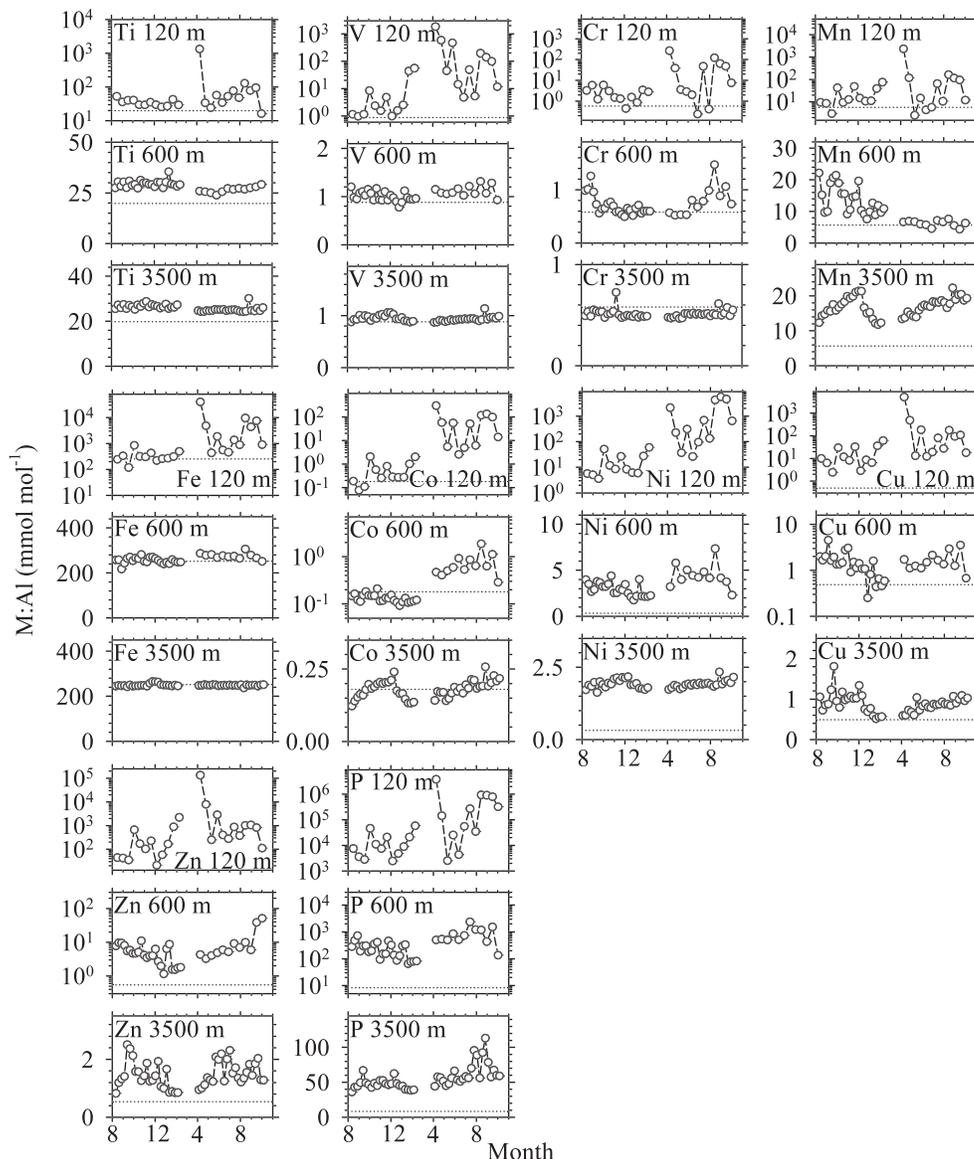
Fig. 5. Al-normalized elemental ratios of the sinking particles at depths of 120, 600, and 3500 m at the SEATS site from August 2004 to October 2005. The horizontal dashed lines represent the element : Al-ratios of the lithogenic particles obtained by Calvert et al. (1993), which are shown in brackets for each element as follows: Ti (20), V (0.88), Cr (0.58), Mn (5.7), Fe (252), Co (0.18), Ni (0.32), Cu (0.49), Zn (0.54), and P (8.3) mmol mol^{-1} Al.

the M : Al ratios during the majority of the sampling time (Fig. 5). Similar results were observed for Cu, Ni, Co, Mn, and P, indicating that the input of nonlithogenic trace metals was still significant in the deeper waters. Unlike Fe or Ti, the intercepts of the linear regression lines for the graphs of the metal flux vs. Al flux did not pass through zero when the Al flux was extrapolated to zero, again showing that lithogenic particles are not the sole nonintracellular trace metal source in deep-water sinking particles (Fig. 6).

Sources of nonlithogenic particulate trace metals in the deep water—Nonlithogenic particulate trace metals in the

sinking particles are known to mainly originate from anthropogenic aerosols in the surface water at the sampling site (Ho et al. 2010b). The particulate trace metals originating from the aerosols may sink down to the deep water and become the major source of nonlithogenic particulate metals in the deep water. This argument is supported by the systematic vertical gradients of the M : Al ratios in the particles collected at the three depths (Fig. 7). When the M : Al ratios of the metals were highly enriched at the shallow depth, their ratios at the two deeper depths were highly elevated (Fig. 7). For example, the M : Al ratios of Zn, Cu, Co, V, and Ni were two to three orders of magnitude higher than the crustal ratios at the surface
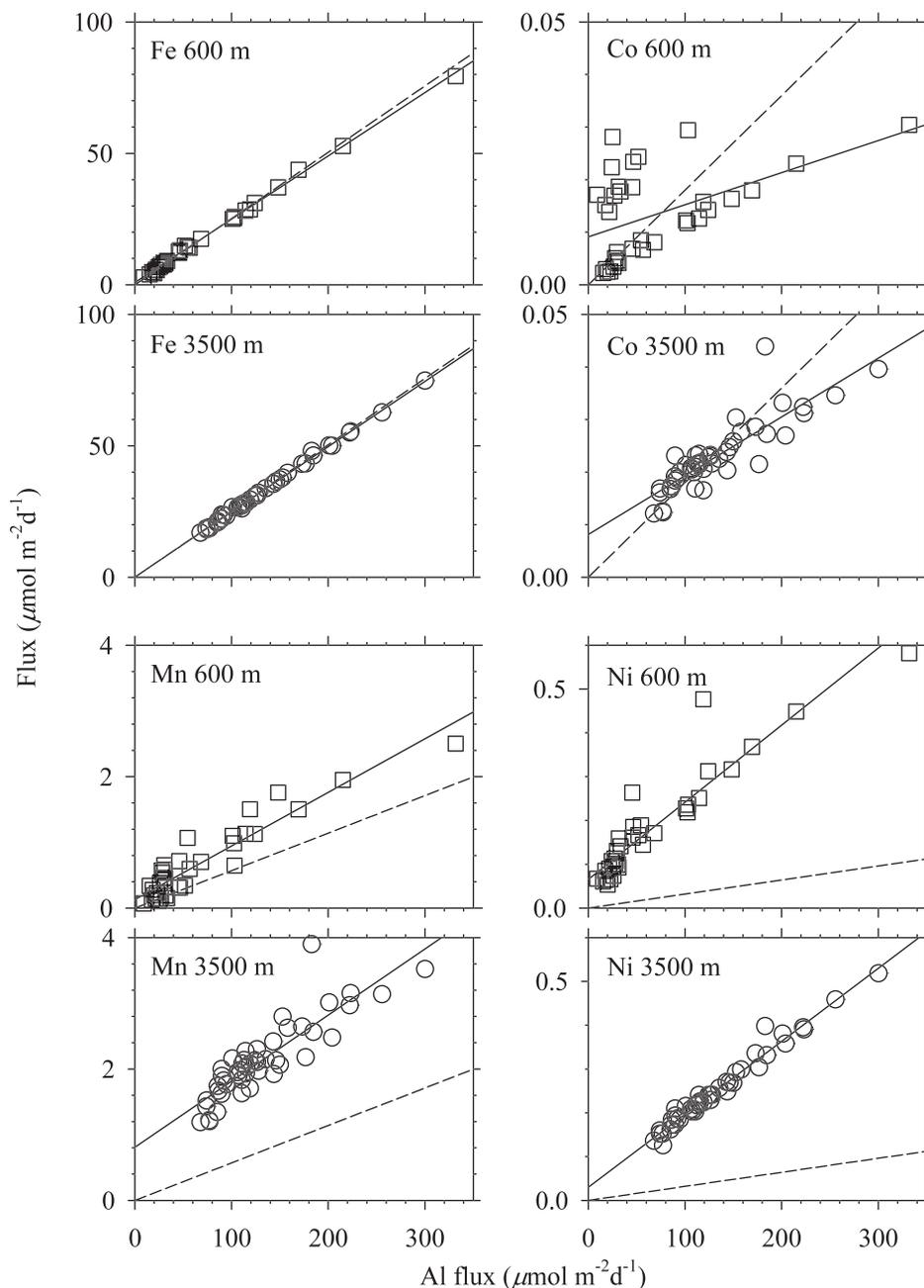
Fig. 6.   Linear correlation of some of the metal fluxes with Al in sediment traps at depths of 600 (open square) and 3500 m (open circle). The solid lines represent linear regression lines, and the dashed lines represent crustal ratios in lithogenic particles (Calvert et al. 1993). With the exception of Fe, Ti, V, and Cr, there were significant positive intercepts on the *y*-axis when the Al flux was extrapolated to zero, in particularly for Zn and Cu (figures not shown).

depth, and the ratios were also relatively high at 600 m, about one order of magnitude higher than the crustal ratios (Fig. 5). Even for Fe and Cr, elevated and correlated M : Al ratios were observed between the surface and the 600-m traps during the second deployment (Fig. 5).

Because most of the particulate trace metals of anthropogenic origin were coupled with sinking organic particles, the remineralization of organic matter would also cause the dissolution of the trace metals of anthropogenic origin in the sinking particles, particularly in the twilight zone. Using Zn as an example, the vertical input of particulate Zn between 120 and 600 m can be estimated from the flux difference between these two depths, which averaged 10 μmol m^{-2} d^{-1} (Tables 1 and 2). The total mass of dissolved Zn in this depth range is obtained by multiplying an average Zn concentration of 3 nmol L^{-1} by 480 m. Without significant horizontal input, the turnover time for particulate Zn of anthropogenic origin to replace the dissolved Zn between these two depths is 144 d. We hypothesize that the transport of trace metals of
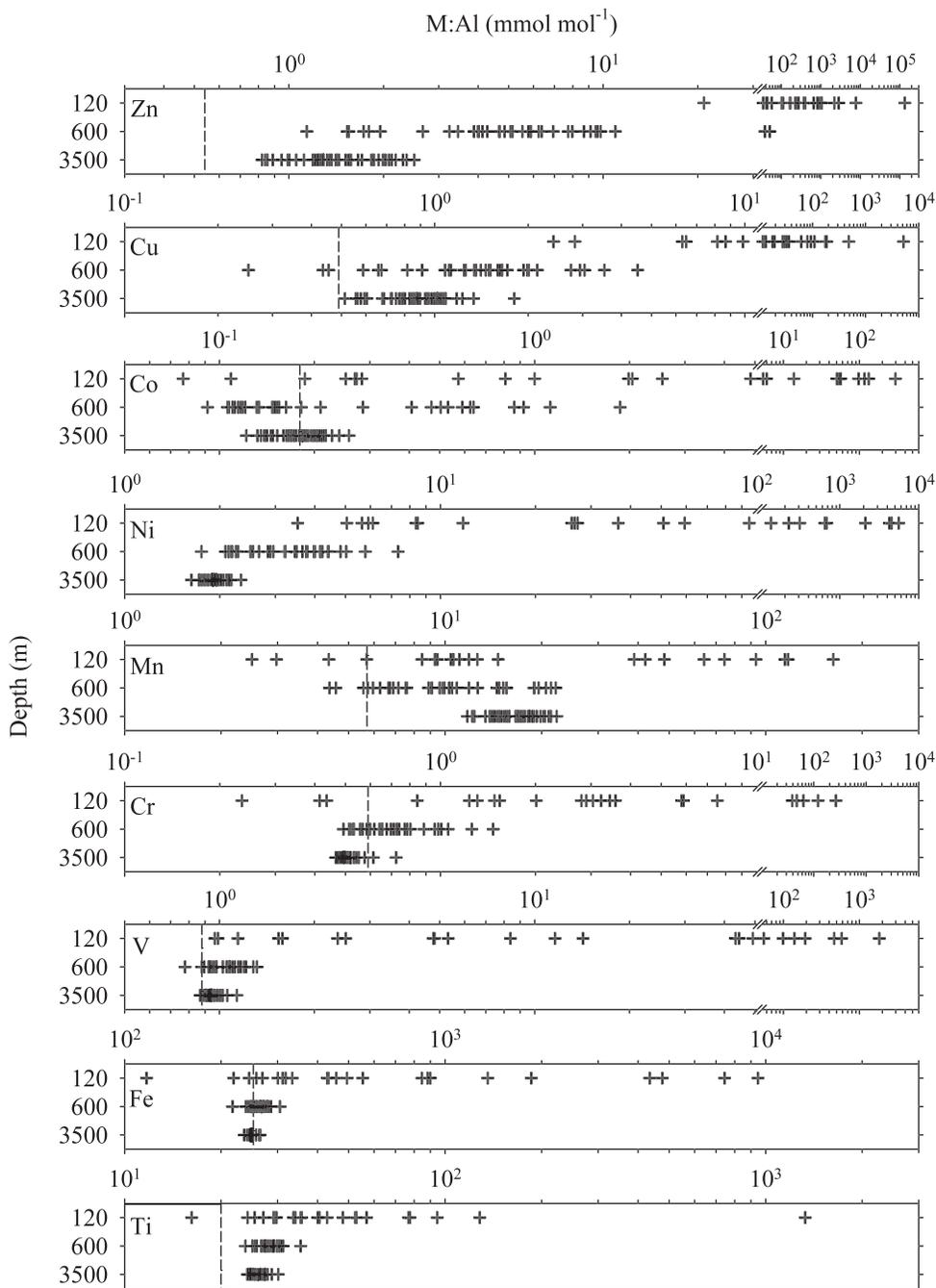
Fig. 7.   Variability comparison of metal-to-Al ratios among the three sampling depths. The ratio scales of the first two orders of magnitude are formatted to be equivalent among the different elements. The ratios of Mn and Co at 3500 m were frequently higher than their ratios at 600 m, indicating a nonlithogenic source below 600 m.

anthropogenic origin to the oceanic twilight zone can be a common phenomenon in the global ocean, particularly for regions with a high aeolian input of anthropogenic aerosols to surface waters. Studies in the Sargasso and Mediterranean Seas indeed observed enriched Zn : Al ratios of sinking particles in deep waters and suggested that the metal may be largely atmospherically derived (Jickells et al. 1984; Grousset et al. 1995; Huang and Conte 2009). A recent

sediment trap study in the top 500 m of the open water in the northern Pacific Ocean also observed highly elevated M : Al ratios for Zn, Cu, Co, and V by comparing to their crustal ratios (Lamborg et al. 2008). If the major source of these highly enriched trace metals in the sediment traps were originally from anthropogenic aerosols transported from the East Asia, it suggests that significant amounts of trace metals of anthropogenic origin, such as Zn, Cu, Co,

and Ni, have been transported to the upper water or even to deep water of the northern Pacific Ocean.

Trace metal isotope composition of seawater and sinking particles may serve as a useful tool to quantitatively estimate the amount of trace metals of anthropogenic origin in oceanic surface and deep waters. With increasing input of anthropogenic aerosols on the global ocean in recent decades, the signals of elemental and isotopic composition of the trace metals may be reflected in the particulate and dissolved trace metals in the whole water columns. Using Zn as an example, we expect that the isotopic composition of particulate Zn in oceanic water columns would be similar to its composition in anthropogenic aerosols because nonlithogenic particulate Zn in the deep water may originate from anthropogenic aerosols. The composition in sinking particles would be distinguishable from its composition in deeper waters, where most of dissolved metals are still nonanthropogenic. The isotope composition of trace metals of anthropogenic origin in surface waters and the composition of dissolved trace metals in deep waters can be used as two end members to estimate the input of trace metals from anthropogenic aerosols.

The sinking particles in the deep water of the sampling site are mainly lithogenic. The suspended particles collected near the mouth of the Pearl River and on the continental shelf of the northern South China Sea are also lithogenic (Ho et al. 2007). Trace metal adsorption on lithogenic particles may thus be an important process generating trace metal–enriched particles in the deep water (Bruland and Lohan 2003). However, the scavenging process is unlikely to be the major cause to enrich some of the nutrient-type trace metals in the particles. The most highly enriched trace metal in the sinking particles is Zn. Zn exhibits a horizontal increase with seawater age in global oceanic deep waters (Bruland and Lohan 2003), indicating that its dissolved form is not prone to be scavenged by sinking particles in oceanic water column.

The formation of authigenic particles in the twilight zone may cause the elevated M : Al ratios for some trace metals in sinking particle of the deep traps. The ratios of Mn and Co to Al at 3500 m displayed a unique seasonal gradient pattern, gradually increasing from August to December in 2004, then declining until February 2005, and increasing again from April to October in 2005 (Fig. 5). Authigenic Mn particles may be formed with the oxidation of reduced Mn below the oxygen minimum zone (OMZ). Reduced Mn may come from lateral transport from the continental shelf or from the reduction of particulate Mn oxides in the OMZ. The OMZ of the South China Sea is located from 600 to 800 m in the water column. The oxidation of reduced Mn may happen below the OMZ and generate particulate Mn in the deeper water (Figs. 5, 6). Indeed, we observed elevated dissolved Mn and Co concentrations between 750 and 1000 m in the water column of the South China Sea and the western Philippine Sea (T. Y. Ho unpubl.) Our recent field study on dissolved trace metals in the continental shelf region of the northern South China Sea from the mouth of the Pearl River to the deep basin showed that the horizontal concentration gradients of Mn reaches

the shelf margin (T. Y. Ho unpubl.). The horizontal transport of dissolved reduced Mn from the continental shelf can be an important external source at the SEATS site. Because the Pearl River's discharge flow peaks in August, the dissolved Mn can be transported to the deep basin and oxidized to form Mn-enriched sinking particles at depths below 600 m.

The relative contributions of the nonlithogenic and lithogenic fractions to sinking particles can also be estimated by mass balance. Without considering authigenic particulate trace metals, the revised equation for the mass balance can be simplified as follows:

$$[M] = b[Al]_{litho} + [M]_{non\text{-}litho}$$

where b is the Al-normalized metal quota in lithogenic particles and $[M]_{non\text{-}litho}$ is the mass of trace metals originating from nonlithogenic sources. The estimated fractions of lithogenic to total trace metals in the sinking particles, calculated by $b[Al]_{litho} : [M]$, are shown in Fig. 8. These fractions were highly variable at the surface, likely due to the pulse inputs of anthropogenic or lithogenic particles from atmospheric forcings. For the lithogenic-type metals (Ti, V, Cr, and Fe), the contribution of anthropogenic components may still occasionally dominate at the surface (Fig. 8). At 600 and 3500 m, the temporal variability in the lithogenic fractions for these elements was small, and their deep-water lithogenic fractions were almost all above 50%, with some even close to 100%. However, the lithogenic fractions for other nutrient-type trace metals, including Mn, Co, Ni, Cu, and Zn, were generally below 50% in deep waters and showed significant temporal variability at 600 m. It should be noted that the lithogenic fraction of Ni in deep waters may be underestimated due to the possible underestimate of Ni : Al ratios in lithogenic particles. Overall, these preliminary estimates indicate that the input of trace metals of nonlithogenic or authigenic origins accounted for a significant fraction for the trace metals in sinking particles of the twilight zone and deep waters.

We extend the schematic model for surface-water trace metal cycling of the South China Sea (Ho et al. 2010b) to the whole water column (Fig. 9). Trace metals in dry or wet aerosols depositing on the surface can either be soluble (M′) or insoluble. Soluble trace metals can either be chelated to an organic ligand (ML) or precipitated as oxyhydroxide metals. Biogenic particles can adsorb lithogenic and anthropogenic particles. Lithogenic particles can be adsorbed onto biogenic particles or sink by themselves. With increasing depth, there is a lower percentage of biogenic particles and a higher percentage of lithogenic particles that make up the total trace metal composition of sinking particles. As shown in Fig. 4, the contribution of intracellular biogenic trace metals was negligible. Except for Mn and Co in the deep-water traps, the trace metals in sinking particles mainly originated either from anthropogenic aerosols or lithogenic particles. With a strong anthropogenic input to the South China Sea in recent decades, some of the trace metals may be transported to the twilight zone and deeper waters. In the upper water
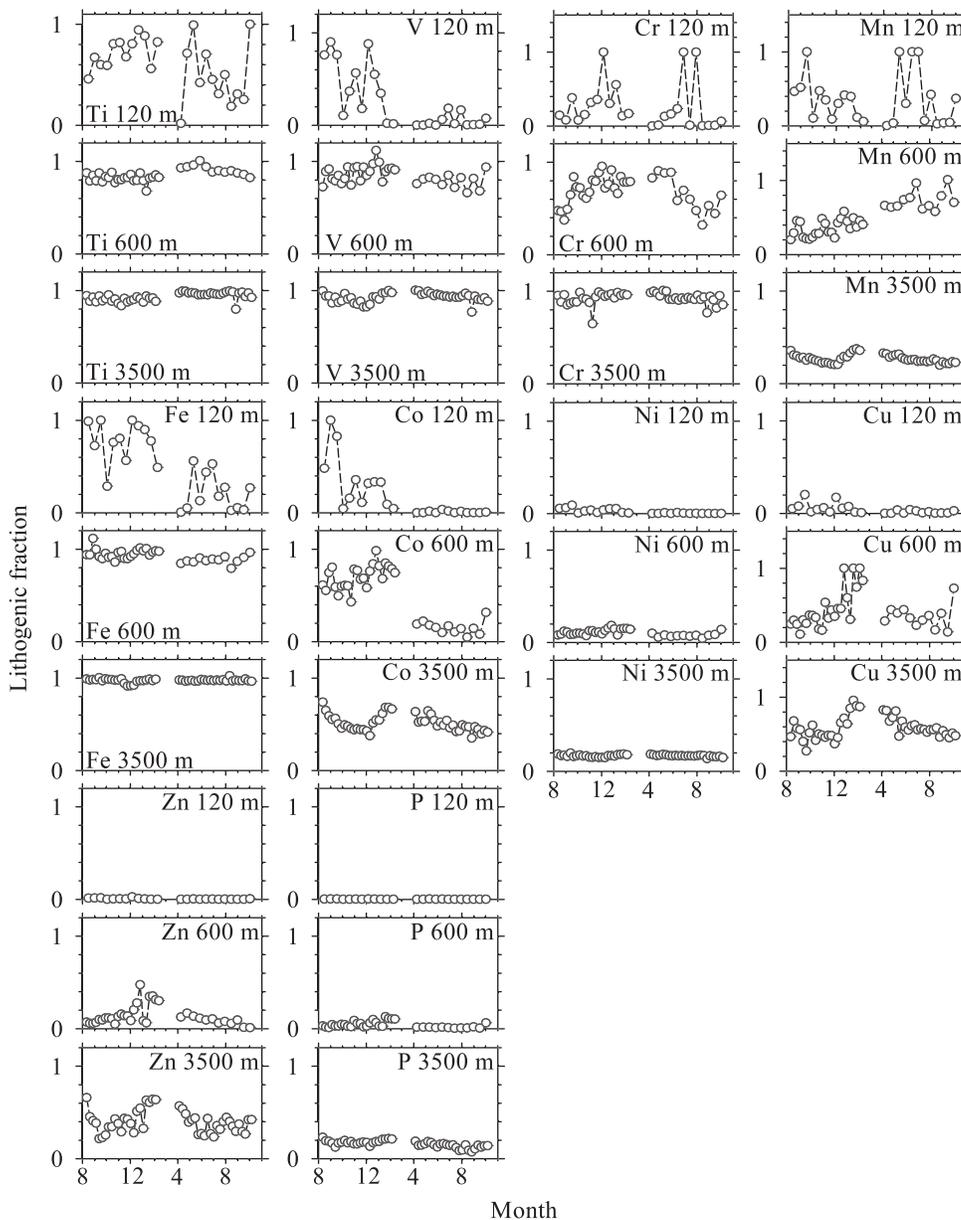
Fig. 8.   The estimated fraction of lithogenic trace metals in the total trace metal content of particles. The number 1 on the y-axis stands for 100% lithogenic fraction. It should be noted that the lithogenic fraction of Ni in the two deeper traps might be underestimated because the Ni : Al ratio in lithogenic particles, 0.32 mmol mol^{-1} Al, may be underestimated (Fig. 5).

column, most of the particulate trace metals were anthropogenic, and many of them were adsorbed and recycled with sinking organic particles. Although lithogenic particles are the major trace metal sources in the sinking particles in the deep water and the fraction increased with depth, significant amounts of anthropogenic and authigenic trace metals were transported from the surface to deeper waters. With increasing inputs from anthropogenic aerosols over large oceanic regions globally, the coupling and transport of anthropogenic trace metals with organic particles has become an important pathway for trace metal cycling not only in the euphotic zone, but also in the twilight zone and deeper waters. Future studies determin-

ing the metal isotope composition of seawater and sinking particles may shed light on the downward input and cycling of aeolian-transported, anthropogenic trace metals in the water column of the global ocean.
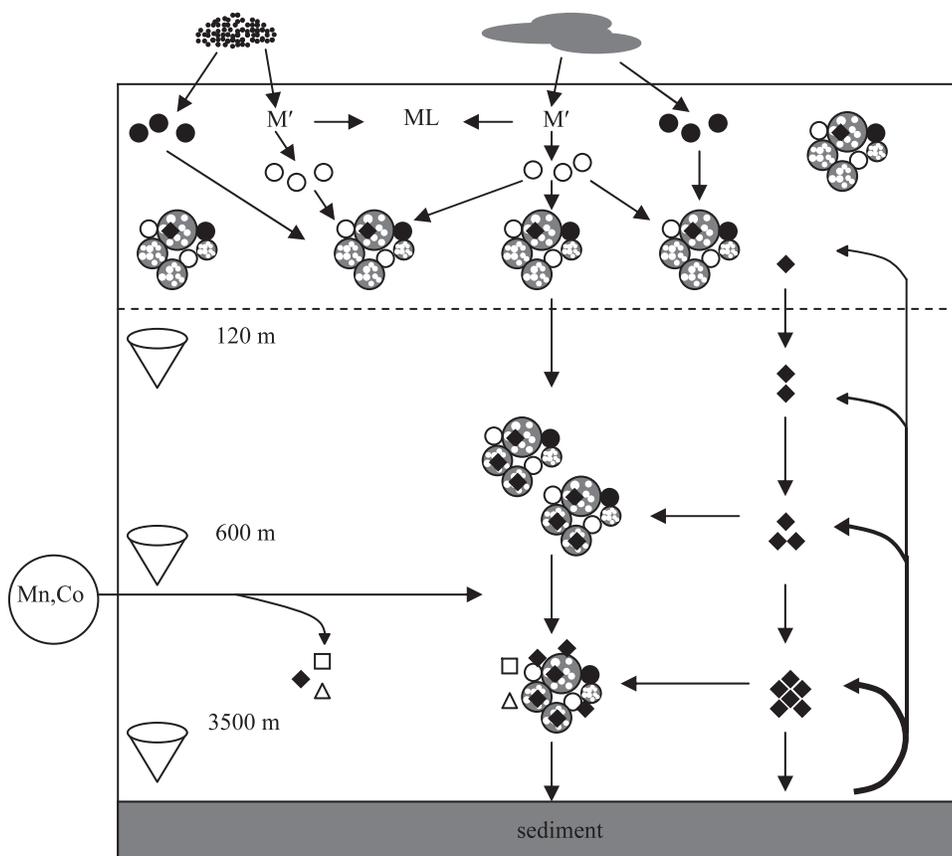
Fig. 9. A schematic model for trace metal transport in the water column of the South China Sea. Anthropogenic trace metals originating either from dry or wet aerosol deposition onto surface waters can either be soluble (M′) or insoluble (solid circle). The soluble trace metals can either be chelated by a soluble organic ligand (ML) or precipitated as hydroxide metals or other chemical precipitates (open circle). Both the insoluble aerosol particles (solid circles) and the precipitates (open circles) may adsorb onto biogenic particles, represented by the porous large circle symbols. Lithogenic particles (solid diamond), which mainly originate from deep water through bottom resuspension or lateral transport of lithogenic particles in the sediment, may be adsorbed onto biogenic particles or sink down by themselves. The concentrations or vertical fluxes of lithogenic particles increase with depth. Mn and Co (open square and triangle) have either a deep water source or a horizontal input from the adjacent continental margin.

References

ANDERSON, R. F., AND G. M. HENDERSON. 2005. GEOTRACES: A global study of the marine biogeochemical cycles of trace elements and their isotopes. Oceanography 18: 76–79.

ANTIA, A. N. 2005. Solubilization of particles in sediment traps: Revising the stoichiometry of mixed layer export. Biogeosciences 2: 189–204, doi:10.5194/bg-2-189-2005

BAKER, E. T., H. B. MILBURN, AND D. A. TENNANT. 1988. Field assessment of sediment trap efficiency under varying flow conditions. J. Mar. Res. 12: 145–152.

BISHOP, J. K. B., J. M. EDMOND, D. R. KETTENS, M. P. BACON, AND W. B. SILKER. 1977. The chemistry, biology, and vertical flux of particulate matter from the upper 400 m of the equatorial Atlantic Ocean. Deep-Sea Res. 24: 511–548.

BRULAND, K. W., AND M. C. LOHAN. 2003. Controls of trace metals in seawater, p. 23–47. In H. Elderfield [ed.], The oceans and marine geochemistry. Elsevier.

———, J. R. DONAT, AND D. A. HUTCHINS. 1991. Interactive influences of bioactive trace metals on biological production in oceanic waters. Limnol. Oceanogr. 36: 1555–1577, doi:10.4319/lo.1991.36.8.1555

BUESSELER, K. O. 1991. Do upper-ocean sediment traps provide an accurate record of particle flux? Nature 353: 420–423, doi:10.1038/353420a0

———, AND OTHERS. 2007. Revisiting carbon flux through the ocean's twilight zone. Science 316: 567–570, doi:10.1126/science.1137959

CALVERT, S. E., T. F. PEDERSEN, AND R. C. THUNELL. 1993. Geochemistry of the surface sediments of the Sulu and South China Seas. Mar. Geol. 114: 207–231, doi:10.1016/0025-3227(93)90029-U

CHEN, Y. L. L. 2005. Spatial and seasonal variations of nitrate-based new production and primary production in the South China Sea. Deep-Sea Res. I **52:** 319–340, doi:10.1016/j.dsr.2004.11.001

COLLIER, R., AND J. EDMOND. 1984. The trace-element geochemistry of marine biogenic particulate matter. Prog. Oceanogr. **13:** 113–199, doi:10.1016/0079-6611(84)90008-9

DEUSER, W. G., P. G. BREWER, T. D. JICKELLS, AND R. F. COMMEAU. 1983. Biological control of the removal of abiogenic particles from the surface ocean. Science **219:** 388–391, doi:10.1126/science.219.4583.388

GROUSSET, F. E., C. R. QUETEL, B. THOMAS, O. F. X. DONARD, C. E. LAMBERT, F. GUILLARD, AND A. MONACO. 1995. Anthropogenic vs. lithogenic origins of trace elements (As, Cd, Pb, Rb, Sb, Sc, Sn, Zn) in water column particles: Northwestern Mediterranean Sea. Mar. Chem. **48:** 291–310, doi:10.1016/0304-4203(94)00056-J

HO, T. Y. 2006. The trace metal composition of marine microalgae in cultures and natural assemblages, p. 271–299. *In* D. V. Subba Rao [ed.], Algal cultures: Analogues of blooms and applications. Science Publishers.

———, C. T. CHIEN, B. N. WANG, AND A. SIRIRAKS. 2010*a*. Determination of trace metals in seawater by an automated flow injection ion chromatograph pretreatment system with ICPMS. Talanta **82:** 1478–1484, doi:10.1016/j.talanta.2010.07.022

———, W. C. CHOU, C. L. WEI, F. J. LIN, G. T. F. WONG, AND H. L. LIN. 2010*b*. Trace metal cycling in the surface water of the South China Sea: Vertical fluxes and sources. Limnol. Oceanogr. **55:** 1807–1820, doi:10.4319/lo.2010.55.5.1807

———, A. QUIGG, Z. V. FINKEL, A. J. MILLIGAN, K. WYMAN, P. G. FALKOWSKI, AND F. M. M. MOREL. 2003. The elemental composition of some marine phytoplankton. J. Phycol. **39:** 1145–1159, doi:10.1111/j.0022-3646.2003.03-090.x

———, L. S. WEN, C. F. YOU, AND D. C. LEE. 2007. The trace-metal composition of size-fractionated plankton in the South China Sea: Biotic versus abiotic sources. Limnol. Oceanogr. **52:** 1776–1788, doi:10.4319/lo.2007.52.5.1776

———, C. F. YOU, W. C. CHOU, S. C. PAI, L. S. WEN, AND D. D. SHEU. 2009. Cadmium and phosphorus cycling in the water column of the South China Sea: The roles of biotic and abiotic particles. Mar. Chem. **115:** 125–133, doi:10.1016/j.marchem.2009.07.005

HONJO, S. 1982. Seasonality and interaction of biogenic and lithogenic particle flux at the Panama Basin. Science **218:** 883–884, doi:10.1126/science.218.4575.883

HUANG, S., AND M. H. CONTE. 2009. Source/process apportionment of major and trace elements in sinking particles in the Sargasso Sea. Geochim. Cosmochim. Acta **73:** 65–90, doi:10.1016/j.gca.2008.08.023

JICKELLS, T. D., W. G. DEUSER, AND A. H. KNAP. 1984. The sedimentation rates of trace elements in the Sargasso Sea measured by sediment trap. Deep-Sea Res. **31:** 1169–1178.

———, AND OTHERS. 2005. Global iron connections between desert dust, ocean biogeochemistry, and climate. Science **308:** 67–71, doi:10.1126/science.1105959

KNAUER, G. A., AND J. H. MARTIN. 1981. Phosphorus-cadmium cycling in northeast Pacific waters. J. Mar. Res. **39:** 65–76.

KUSS, J., AND K. KREMLING. 1999. Spatial variability of particle associated trace elements in near-surface waters of the North Atlantic (30°N/60°W to 60°N/2°W), derived by large-volume sampling. Mar. Chem. **68:** 71–86, doi:10.1016/S0304-4203(99)00066-3

LAMBORG, C. H., K. O. BUESSELER, AND P. J. LAM. 2008. Sinking fluxes of minor and trace elements in the North Pacific Ocean measured during the VERTIGO program. Deep-Sea Res. II **55:** 1564–1577, doi:10.1016/j.dsr2.2008.04.012

LIN, I. I., J. P. CHEN, G. T. F. WONG, C. W. HUANG, AND C. C. LIEN. 2007. Aerosol input to the South China Sea: Results from the MODerate resolution imaging spectro-radiometer, the quick scatterometer, and the measurements of pollution in the troposphere sensor. Deep-Sea Res. II **54:** 1589–1601, doi:10.1016/j.dsr2.2007.05.007

LIU, Z. F., C. LEE, AND S. G. WAKEHAM. 2006. Effects of mercuric chloride and protease inhibitors on degradation of particulate organic matter from the diatom *Thalassiosira pseudonana*. Org. Geochem. **37:** 1003–1018, doi:10.1016/j.orggeochem.2006.05.013

MARTIN, J. H. 1990. Glacial-interglacial CO_2 change: The iron hypothesis. Paleoceanography **5:** 1–13, doi:10.1029/PA005i001p00001

———, G. A. KNAUER, D. M. KARL, AND W. W. BROENKOW. 1987. VERTEX: Carbon cycling in the north Pacific. Deep-Sea Res. **34:** 267–285.

NORISUYE, K., M. EZOE, S. NAKATSUKA, S. UMETANI, AND Y. SOHRIN. 2007. Distribution of bioactive trace metals (Fe, Co, Ni, Cu, Zn and Cd) in the Sulu Sea and its adjacent seas. Deep-Sea Res. II **54:** 14–37, doi:10.1016/j.dsr2.2006.04.019

NRIAGU, J. O., AND J. M. PACYNA. 1988. Quantitative assessment of worldwide contamination of air, water and soils by trace-metals. Nature **333:** 134–139, doi:10.1038/333134a0

PACE, M. L., G. A. KNAUER, D. M. KARL, AND J. H. MARTIN. 1987. Primary production, new production and vertical flux in the eastern Pacific Ocean. Nature **325:** 803–804, doi:10.1038/325803a0

POHL, C., A. LOFFLER, AND U. HENNINGS. 2004. A sediment trap flux study for trace metals under seasonal aspects in the stratified Baltic Sea (Gotland Basin; 57°19.20′N; 20°03.00′E). Mar. Chem. **84:** 143–160, doi:10.1016/j.marchem.2003.07.002

QU, T., J. B. GIRTON, AND J. A. WHITEHEAD. 2006. Deepwater overflow through Luzon Strait. J. Geophys. Res. **111:** C01002, doi:10.1029/2005JC003139

SEDWICK, P. N., E. R. SHOLKOVITZ, AND T. M. CHURCH. 2007. Impact of anthropogenic combustion emissions on the fractional solubility of aerosol iron: Evidence from the Sargasso Sea. Geochem. Geophys. Geosyst. **8:** Q10Q06, doi:10.1029/2007GC001586

SHOLKOVITZ, E. R., P. N. SEDWICK, AND T. M. CHURCH. 2009. Influence of anthropogenic combustion emissions on the deposition of soluble aerosol iron to the ocean: Empirical estimates for island sites in the North Atlantic. Geochim. Cosmochim. Acta **73:** 3981–4003, doi:10.1016/j.gca.2009.04.029

TAYLOR, S. R. 1964. Abundance of chemical elements in the continental crust: A new table. Geochim. Cosmochim. Acta **28:** 1273–1285, doi:10.1016/0016-7037(64)90129-2

TSENG, C. M., G. T. F. WONG, I. I. LIN, C. R. WU, AND K. K. LIU. 2005. A unique seasonal pattern in phytoplankton biomass in low-latitude waters in the South China Sea. Geophys. Res. Lett. **32:** L08608, doi:10.1029/2004GL022111

TUREKIAN, K. K. 1977. Fate of metals in oceans. Geochim. Cosmochim. Acta **41:** 1139–1144, doi:10.1016/0016-7037(77)90109-0

WEN, L. S., K. T. JIANN, AND P. H. SANTSCHI. 2006. Physicochemical speciation of bioactive trace metals (Cd, Cu, Fe, Ni) in the oligotrophic South China Sea. Mar. Chem. **101:** 104–129, doi:10.1016/j.marchem.2006.01.005

WHITFIELD, M., AND D. R. TURNER. 1987. The role of particles in regulating the composition of sea water, p. 457–493. *In* W. Stumm [ed.], Aquatic surface chemistry: Chemical processes at the particle–water interface. Wiley-Interscience.

WONG, G. T. F., T. L. KU, M. MULHOLLAND, C. M. TSENG, AND D. P. WANG. 2007. The southeast Asian time-series study (SEATS) and the biogeochemistry of the South China Sea—an overview. Deep-Sea Res. II **54:** 1434–1447, doi:10.1016/j.dsr2.2007.05.012

WU, C. R., T. Y. TANG, AND S. F. LIN. 2005. Intra-seasonal variation in the velocity field of the northeastern South China Sea. Cont. Shelf Res. **25:** 2075–2083, doi:10.1016/j.csr.2005.03.005